

SURGERY FOR ACQUIRED CARDIOVASCULAR DISEASE

RE-CREATION OF SINUSES IS IMPORTANT FOR SPARING THE AORTIC VALVE: A FINITE ELEMENT STUDY

K. Jane Grande-Allen, PhD^a
Richard P. Cochran, MD^b
Per G. Reinhall, PhD^c
Karyn S. Kunzelman, PhD^b

Objective: The treatment of choice for aortic valve insufficiency due to root dilatation has become root replacement with aortic valve sparing. However, root replacement with a synthetic graft may result in altered valve stresses. The purpose of this study was to compare the stress/strain patterns in the spared aortic valve in different root replacement procedures by means of finite element modeling.

Methods: Our finite element model of the normal human root and valve was modified to simulate and evaluate three surgical techniques: (1) “cylindrical” graft sutured below the valve at the anulus, (2) “tailored” graft sutured just above the valve, and (3) “pseudosinus” graft, tailored and sutured below the valve at the anulus. Simulated diastolic pressures were applied, and stresses and strains were calculated for the valve, root, and graft. Leaflet coaptation was also quantified.

Results: All three root replacement models demonstrated significantly altered leaflet stress patterns as compared with normal patterns. The cylindrical model showed the greatest increases in stress (16%-173%) and strain (10%-98%), followed by the tailored model (stress +10%-157%, strain +9%-36%). The pseudosinus model showed the smallest increase in stress (9%-28%) and strain (2%-31%), and leaflet coaptation was closest to normal.

Conclusion: Valve-sparing techniques that allow the potential for sinus space formation (tailored, pseudosinus) result in simulated leaflet stresses that are closer to normal than the cylindrical technique. Normalized leaflet stresses in the clinical setting may result in improved longevity of the spared valve. (J Thorac Cardiovasc Surg 2000;119:753-63)

From the Department of Biomedical Engineering, Cleveland Clinic Foundation, Cleveland, Ohio^a; Division of Cardiothoracic Surgery, University of Wisconsin, Madison, Wis^b; and Department of Mechanical Engineering, University of Washington, Seattle, Wash.^c

This research was performed in the Department of Bioengineering and the Division of Cardiothoracic Surgery at the University of Washington.

Supported by the Whitaker Foundation and the National Partnership for Advanced Computational Infrastructure.

Received for publication May 6, 1999; revisions requested Aug 26, 1999; revisions received Oct 11, 1999; accepted for publication Nov 23, 1999.

Address for reprints: Karyn S. Kunzelman, PhD, University of Wisconsin, CSC H4/368, 600 Highland Ave, Madison, WI 53792-3236 (E-mail: karynk@surgery.wisc.edu).

Copyright © 2000 by The American Association for Thoracic Surgery.

0022-5223/2000 \$12.00 + 0 12/1/104582

[doi.10.1067/mtc.2000.104582](https://doi.org/10.1067/mtc.2000.104582)

In recent years, synthetic vascular grafts have been used in “valve-sparing” operations for aortic valve incompetence that is due to aortic root dilatation without significant valvular degeneration. These operative procedures are designed to restore aortic valve competence by excising the dilated aortic root and replacing it with an appropriately sized cylindrical polyester graft sutured either below the valve anulus^{1,2} or above the leaflet attachments.^{3,4} The goal of these procedures is to preserve the native valve, avoid life-long anticoagulation, and restore normal valve function by recreating the normal anatomic root environment.

Although early and midterm results of such procedures have been reported favorably,⁴ true long-term results are not yet available; thus the durability of these procedures is not known. This durability is likely dependent on the stress state of the aortic valve

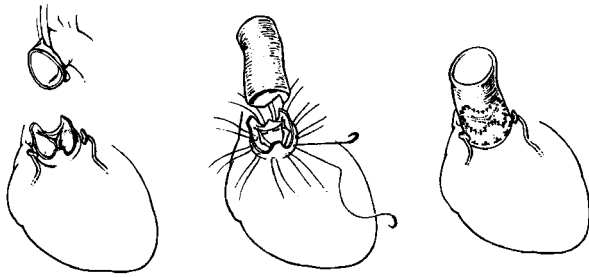


Fig 1. The valve-sparing procedure represented by the “cylindrical” model. The dilated aortic root and sinuses are excised and a cylindrical polyester graft is sutured below the annulus. (Adapted from David TE: Aortic valve repair in patients with Marfan syndrome and ascending aorta aneurysms due to degenerative disease. *J Card Surg* 1994;9[Suppl]:182-7. Copyright 1994 by Futura Publishing Company, Inc. Reprinted with permission of Futura Publishing Company, Inc.)

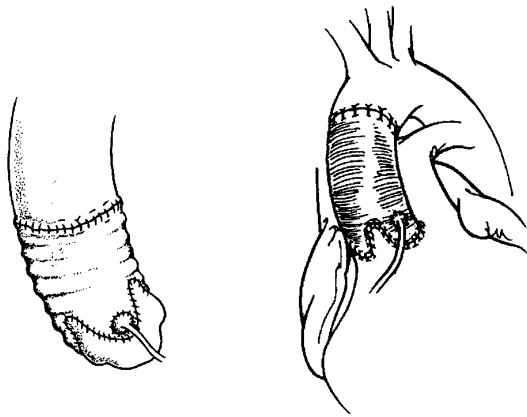


Fig 2. The valve-sparing procedures represented by the “tailored” model. The dilated aortic root is resected, and the cylindrical graft is tailored and sutured above the leaflet attachments. The *left panel* shows the procedure as described by Sarsam and Yacoub and the *right panel* as described by David. (Adapted from Sarsam MA, Yacoub Y: Remodeling of the aortic valve annulus. *J Thorac Cardiovasc Surg* 1993;105:435-8. Copyright 1993 by Mosby-Year Book. Reprinted with permission of Mosby, Inc. Adapted from David TE: Aortic valve repair in patients with Marfan syndrome and ascending aorta aneurysms due to degenerative disease. *J Card Surg* 1994;9[Suppl]:182-7. Copyright 1994 by Futura Publishing Company, Inc. Reprinted with permission of Futura Publishing Company, Inc.)

leaflets and their ability to function normally within the artificial root environment. Because the compliant tissue properties and rounded shape of the native aortic root promote the normal function of valve,^{5,6} root replacement with a cylindrically shaped and relatively stiffer⁷ polyester graft would affect the resulting

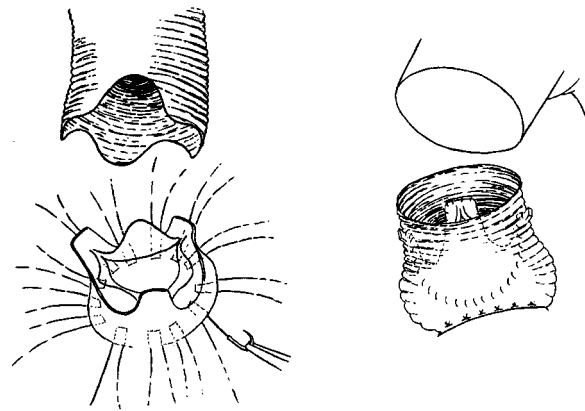


Fig 3. The valve-sparing procedure represented by the “pseudosinus” model. The cylindrical graft is “scalloped” and then sutured in a plane below the annulus, so that the resulting bulging of the graft results recreates the sinuses. The graft configuration is Cochran’s modification to the original David procedure. (Adapted from Cochran RP, Kunzelman KS, Eddy AC, Hofer BO, Verrier ED. Modified conduit preparation creates a pseudosinus in an aortic valve-sparing procedure for aneurysm of the ascending aorta. *J Thorac Cardiovasc Surg* 1995;109:1049-57; discussion 1057-8. Copyright 1995 by Mosby-Year Book. Reprinted with permission of Mosby, Inc.)

levels of stress and strain in the spared aortic valve leaflets. Furthermore, we suspect that the combined function of the native valve and the root graft may be different from the combined function of the native valve and the normal root.

Although the theoretical advantages and disadvantages of differing valve-sparing procedures have been examined,⁸ no systematic study of the resulting influence on the stresses of the spared valve has yet been conducted. To perform such a study, we have developed a fully 3-dimensional, anatomically realistic finite element mathematical model of the aortic root and valve. As opposed to prior finite element models of the aortic valve,^{9,10} our model does not presume any a priori symmetry, and it includes the root walls with their sinuses of Valsalva and their respective coronary ostia. The objective of this investigation was to model and evaluate three potential surgical options for restoring valve competence via aortic root replacement by analyzing the functional and closing characteristics of the simulated spared aortic valve.

Methods

To investigate the replacement of the root with a vascular graft in three different aortic valve-sparing surgical procedures, we used finite element mathematical models to evaluate replacement of the aortic root with three different poly-

ester vascular graft shapes. The first model (cylindrical) simulated a procedure (Fig 1) in which the sinus walls were excised and a cylindrical graft was sutured below the anulus.¹ The second model (tailored) simulated a “neo-sinus” procedure (Fig 2) in which the graft was tailored and sutured above the leaflet attachments,^{3,4} with the potential for sinus accommodation. The third model (pseudosinus) simulated a procedure (Fig 3) in which the graft was “scalloped” and then sutured in a plane below the anulus,² so that the resulting bulging of the graft recreated the sinuses. The results of these models were compared to that of our normal model of the aortic root and valve. The primary methods have been described in detail previously¹¹ and are summarized here.

Normal model geometry and element development.

Finite element analysis is a computational technique in which an object with a complicated structure is divided into smaller sections, termed elements, that are interconnected by common points, termed nodes. This discretization enables the use of algebraic equations to describe the individual structural state at each node. The solution of the system of equations yields the displacement, stress, and strain at any point in the entire object.¹²

Our finite element model was developed with the use of ANSYS software (version 5.3, ANSYS Inc, Canonsburg, Pa) run on a DEC Alphastation 400 4/233 workstation (Digital Equipment Corporation, Maynard, Mass). Magnetic resonance imaging of normal human aortic valve and root specimens was used to establish the geometry for the model. Because assemblies of triangular shell elements are well suited to reproduce curved geometries, we selected the six-noded triangular shell element to take advantage of its capacity for linearly varying stress and strain.¹² Preliminary benchmark models (simple structural analysis problems in which the solution is known) using these same elements at the same density as in our root/valve model had stresses, strains, and displacements with a numerical accuracy within less than 0.5%. We created 5000 elements to represent the aortic root and 1815 elements for the three valve leaflets.

Element thicknesses and material properties. The normal aortic root thickness values were measured directly from the magnetic resonance images of the root wall. The thicknesses of the unpressurized valve leaflets were determined from published data.^{13,14} The anisotropic material properties of both tissues were also calculated from published stress-strain data,¹⁵⁻¹⁷ including a Poisson ratio of 0.45 to account for tissue incompressibility.¹⁸ To represent the pliability of the aortic valve leaflets,¹⁹ the bending stiffness of the shell elements in the valve was reduced by 98.5% (method detailed previously in an appendix¹¹). The polyester material (polyethylene terephthalate) was assumed to be isotropic with a Poisson ratio of 0.3,²⁰ an elastic modulus of 7840 kPa (based on the range of stiffnesses reported in the literature²¹⁻²³), fabric thickness²⁴ of 0.305 mm, and a crimp angle of 40°.

Modifications for graft models. Each graft model required modification of our established model,¹¹ which incorporates normal aortic root shape and element properties. First, the cylindrical graft model was created by removing the

root elements located above the valve attachment edge from the normal root geometry, then simulating a 24-mm diameter graft cylinder with inclusion of the remnant aortic wall (Fig 4, *a* and *b*). The effective material properties of a crimped, woven polyester graft were assigned to the cylinder. In the areas where the remnant aortic wall was present within the graft (in yellow, Fig 4, *b*), the elements were assigned material properties of the combined graft and aortic wall.

Next, for the tailored graft model, the root elements above the valve attachment edge were similarly removed, and a 24 mm-diameter polyester cylinder was simulated above the remainder of the root (Fig 4, *c* and *d*) in an edge-to-edge fashion. Thus, in remnant aortic wall areas (in yellow, Fig 4, *d*), the elements were assigned material properties of the aortic wall alone.

Finally, to represent the sinus shape that would optimally be attained by a pseudosinus model, the same root elements were again removed and replaced by a polyester cylinder above the sinotubular junction (Fig 4, *e* and *f*). Below the sinotubular junction, sinus-shaped polyester root walls were simulated, with inclusion of the remnant aortic wall. The elements representing the remnant aortic wall within the graft (in yellow, Fig 4, *f*) were assigned material properties of the combined graft and aortic wall. The curved shape of the sinus walls in the model is described by the following logistic function:

$$z = a + 4b \exp \left(\frac{\left(\frac{-(x-s)}{d} \right)}{\left(1 + \exp \left(\frac{-(x-c)}{d} \right) \right)^2} \right) + 4e \exp \left(\frac{\left(\frac{-(y-f)}{g} \right)}{\left(1 + \exp \left(\frac{-(y-f)}{g} \right) \right)^2} \right) + 16h \exp \left(\frac{\left(\frac{-(x-s)}{d} \right) \left(\frac{(y-f)}{g} \right)}{\left(1 + \exp \left(\frac{-(x-c)}{d} \right) \right)^2 \left(1 + \exp \left(\frac{-(y-f)}{g} \right) \right)^2} \right)$$

where $a = -0.215$, $b = -0.302$, $c = 0.448$, $d = 0.290$, $e = 0.545$, $f = -0.007$, $g = 0.438$, and $h = 0.637$.

To simulate the anastomosis of the coronary ostia “buttons” to the root graft, we repositioned the right and left coronary ostia at the center of their respective sinuses. In addition, the thickness and stiffness of the graft were added to the ostia elements closest to the root to simulate the suturing of the ostial button to the graft.

Boundary conditions. Geometric boundary constraints were assigned to all models in exactly the same manner. First, contact elements were incorporated into the coapting leaflet surface to allow for the free sliding of leaflet surfaces and to prevent the leaflets from passing through each other or through the root wall. Second, the lowest layer of the aortic root base was restricted to in-plane displacement. Third, the physiologic longitudinal stretch found normally in the aorta

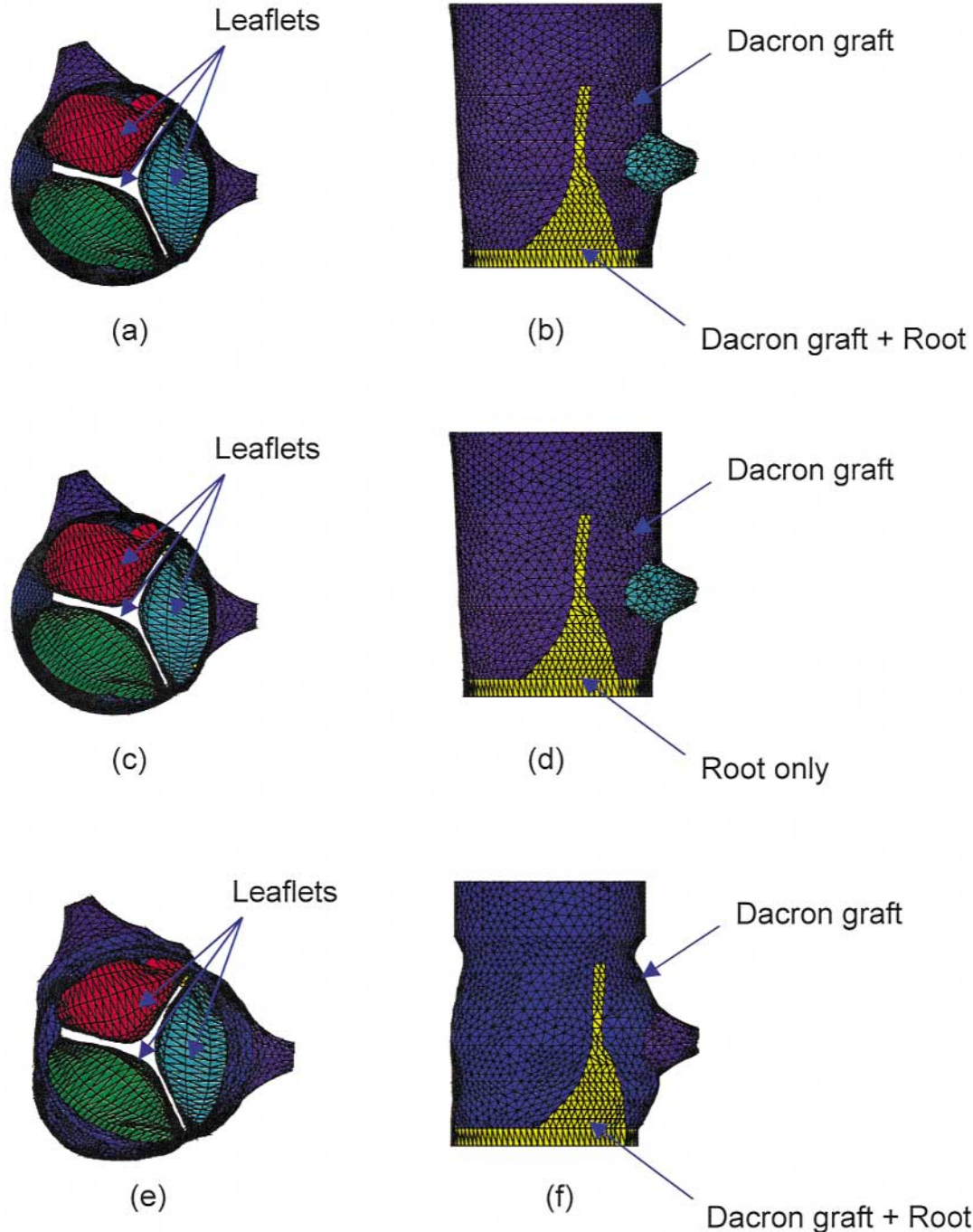


Fig 4. Geometry for the finite element models. Cylindrical graft models: **a**, top view; **b**, side view. The purple elements represent the polyester graft material above the leaflet attachment line. The yellow elements represent both the graft and the included root remnant. Tailored graft models: **c**, top view; **d**, side view. The purple elements represent the polyester graft material above the leaflet attachment line. The yellow elements represent the root remnant alone. Optimized sinus graft models: **e**, top view; **f**, side view. The blue elements represent the polyester graft material above the leaflet attachment line, and the yellow elements represent both the graft and the included root remnant.

and other arteries²⁵ was imposed by applying a tension boundary condition at the top of the simulated ascending aorta and at the distal ends of the coronary ostia.

Pressure loading pattern. To model the early diastolic loading of the aortic valve and root/graft, we applied simulat-

ed physiologic pressures to the valve and root/graft structure in two phases. In the first phase, the aortic root (or root graft) alone was pressurized in a linearly increasing manner until it reached the end-systolic aortic pressure level. In the second phase, physiologic pressures were applied to the aortic valve,

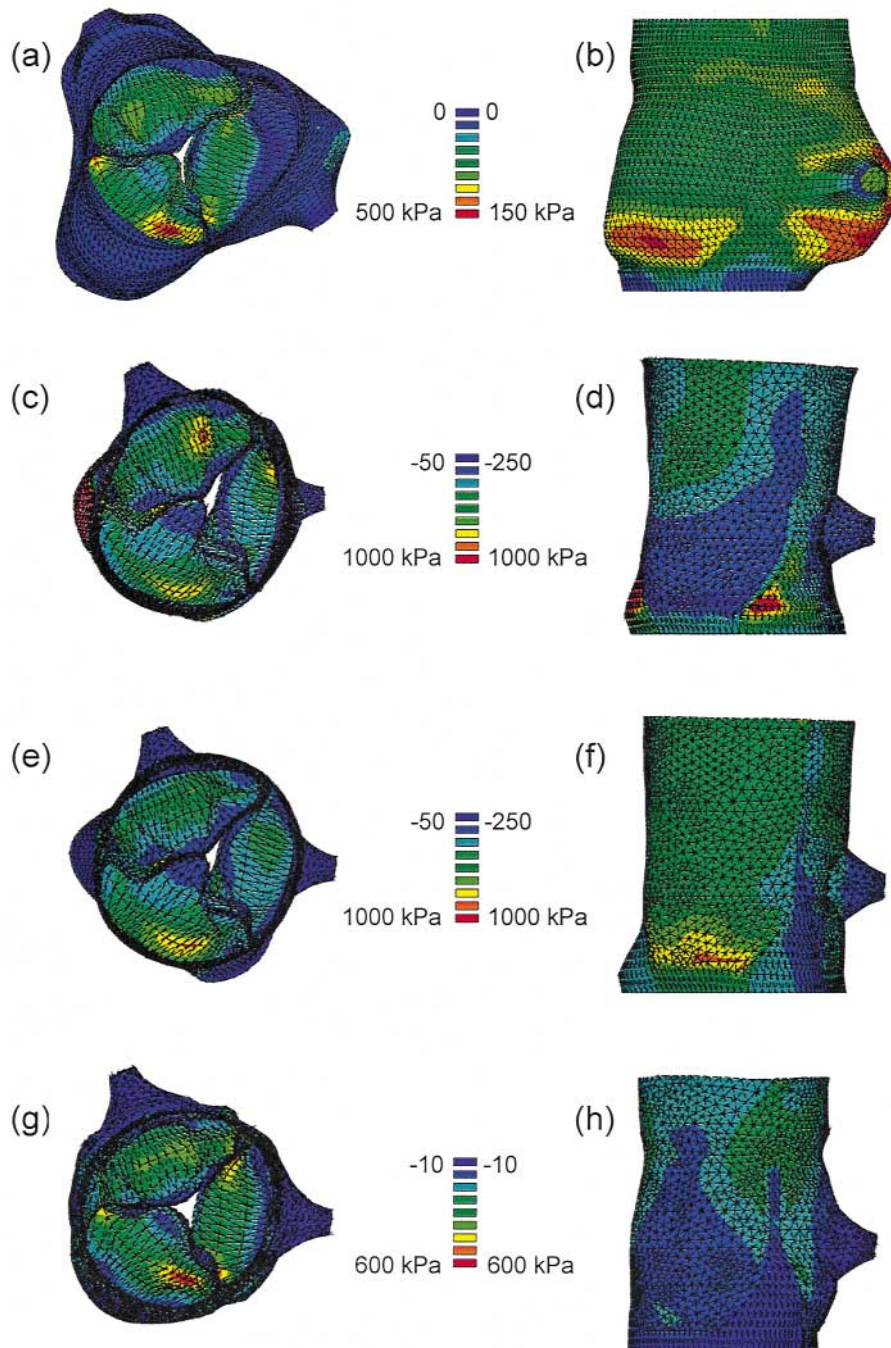


Fig 5. Stress contours of the valve and root in the root graft models: **a**, normal root model, top view; **b**, normal root model, side view; **c**, cylindrical graft model, top view; **d**, cylindrical graft model, side view; **e**, tailored graft model, top view; **f**, tailored graft model, side view; **g**, pseudosinus graft model, top view; **h**, pseudosinus graft model, side view.

to the root or root graft, and to the region of the root underneath the valve. These pressures were calculated from aortic and left ventricular pressures and an assumed average negative chest pressure of 5 mm Hg. Loading started at end-systole, just after valve closure, and finished at the end of left

ventricular isovolumic relaxation, when peak pressure across the valve was reached.

Solution method. The models were solved on the DEC Alphastation workstation or on the Cray J90 supercomputer system (Silicon Graphics, Inc, Mountain View, Calif) at the

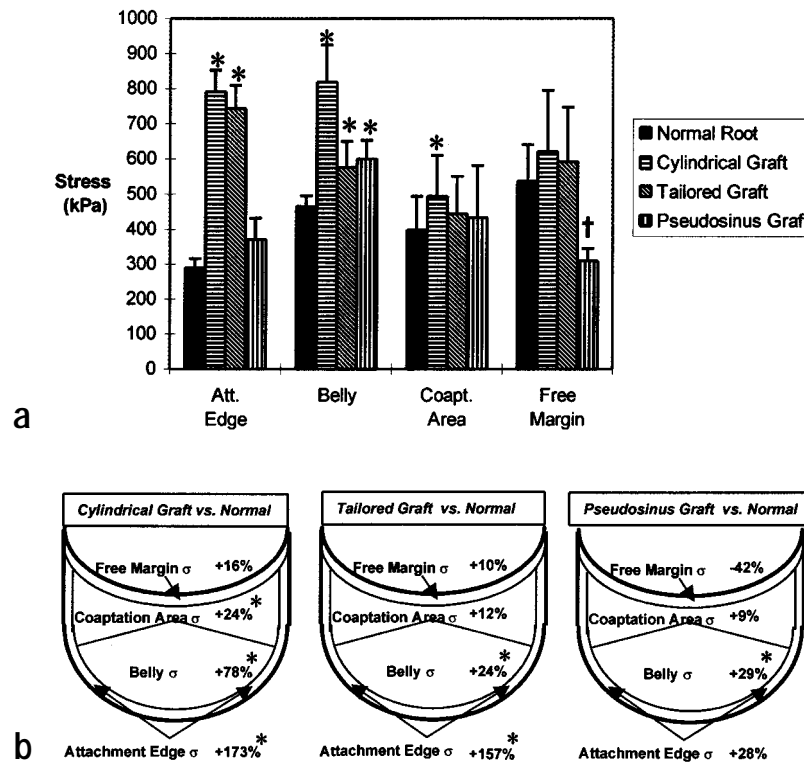


Fig 6. a, Aortic valve regional stresses in the normal aortic root and clinical valve-sparing models. * $P = .0001$ and † $P = .0005$ indicate significant difference as compared with the normal root model. **b**, Schematics of altered leaflet stress patterns in the graft models as compared with normal.

Texas Advanced Computing Center. The solution was performed iteratively by dividing the pressure loading phases into a number of equal steps (81 aortic root preliminary steps + 118 physiologic root/valve steps = 199 total).

Output analysis. Stress and strain in the valve and root or root graft were examined at the end of physiologic loading. (Stress [σ] is defined as the force [F] applied to the tissue divided by cross-sectional area [A], ie, $\sigma = F/A$. Strain [ϵ] is defined as percent extension of the tissue, ie, $\epsilon = \Delta L/L_0$, where ΔL is change in length and L_0 is original length.) For both the leaflets and root sinuses, the magnitude and location of the principal tensile stresses and strains were recorded. Regional magnitudes were calculated by grouping sets of elements to define specific model components (belly, coaptation area, free margin, attachment edge, annular sinus wall, sinotubular junction sinus wall) and then analyzing those components to determine the average, standard deviation, maximum, and minimum values. In addition, the "peak average" was calculated, which was the average value of the 5% of elements with the highest values (the peak standard deviation was calculated similarly). The coaptation area, defined as the percentage of leaflet area contacting the adjacent leaflet surfaces, was also examined throughout the preliminary root loading and subsequent physiologic root/valve loading phas-

es. The stress and strain results were compared by means of analysis of variance to determine significant differences with respect to the graft type.

Results

Stress, strain, and coaptation. Leaflet stress and strain magnitudes were altered in all clinical graft models, particularly at the attachment edge, as compared with the normal root model (Figs 5-7). The cylindrical graft demonstrated the greatest alterations, and slight improvements were noted with the tailored graft. The pseudocusinus graft resulted in stress and strain patterns that were the closest to normal of all three models.

As a result of the altered stress and strain patterns in the leaflets, as well as the decreased graft stiffness, leaflet coaptation was also affected. The average percent valve coaptation was 27% for the normal root model, 32% for the cylindrical, 35% for the tailored, and 29% for the pseudocusinus graft.

An analysis of average directional strains in these graft model leaflets demonstrated that the valve was

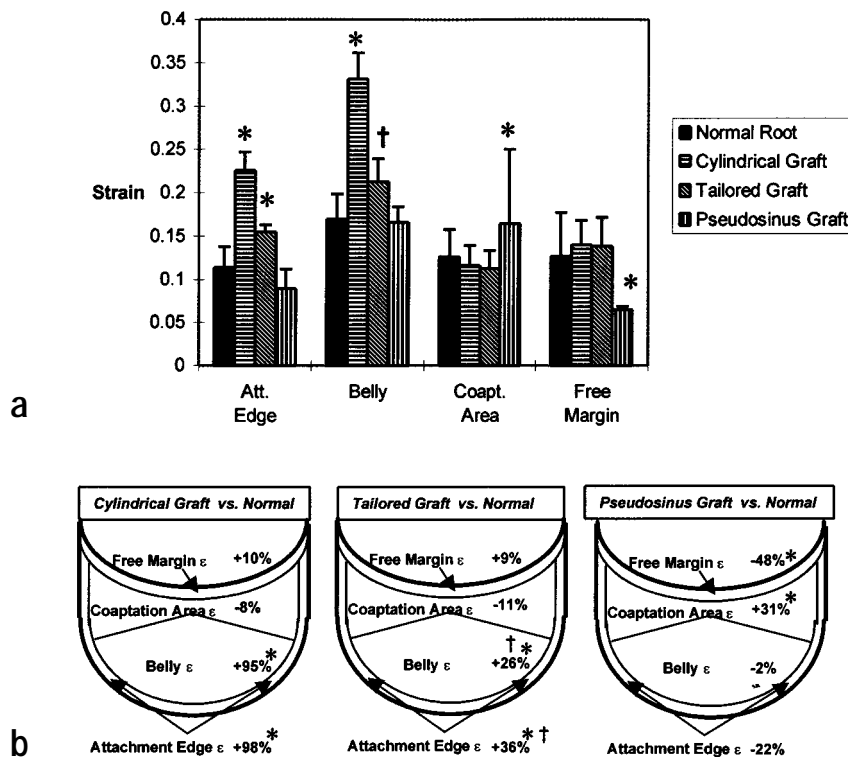


Fig 7. a, Aortic valve regional strains in the normal aortic root and clinical valve-sparing models. $*P = .0001$ and $†P = .001$ indicate significant difference as compared with the normal root model. **b,** Schematics of altered leaflet strain patterns in the graft models as compared with normal.

displaced downward toward the left ventricular outflow tract to a greater extent than in the normal model. In all the graft models, there was much less leaflet strain in the radial direction than in the longitudinal direction, with radial/longitudinal strain ratios of 0.29:1, 0.18:1, and 0.29:1, respectively, in the cylindrical, tailored, and pseudosinus models. This situation is opposite that found in the normal root model, in which there was more leaflet radial strain than longitudinal strain, with a ratio of 1.94:1.

Graft stress and strain. For all models, the grafts maintained their approximate original shapes even at the peak aortic pressure (as shown in Fig 5). In the cylindrical graft model, the graft had 1081% higher stress ($P = .0001$) and 86% lower strains ($P = .0001$) as compared with the normal aortic root (Fig 8). In the tailored graft model, the graft had 517% higher stress ($P = .0001$) and 90% lower strain ($P = .0001$). The pseudosinus graft had 191% higher stress ($P = .0001$) and 96% lower strain ($P = .0001$).

Root-valve relationship. The stresses in the annular region of the cylindrical, tailored, and pseudosinus

grafts were transferred to the valve leaflets. This transfer was evidenced by the lower stresses in the annular region of graft wall as compared with the sinotubular junction region of graft wall (the opposite of the pattern in the normal root model) and the increased stress magnitudes in the leaflet attachment edge and belly as compared with the normal root model.

Discussion

Study limitations. As with any modeling study, our model encompasses inherent limitations, as described previously.¹¹ First, we chose to model only the rapid final closing phase of the valve leaflets, as tensile stresses are highest during this period. Second, the model material properties were assumed to be constant in the physiologic range of the stress-strain curve. This choice was partly software-dependent: ANSYS finite element software does not permit both anisotropic and nonlinear material behavior. Therefore the stress and strain results in the model may be lower than in the actual tissues. However, we are simulating diastolic function only, where the valve and aortic tissue has

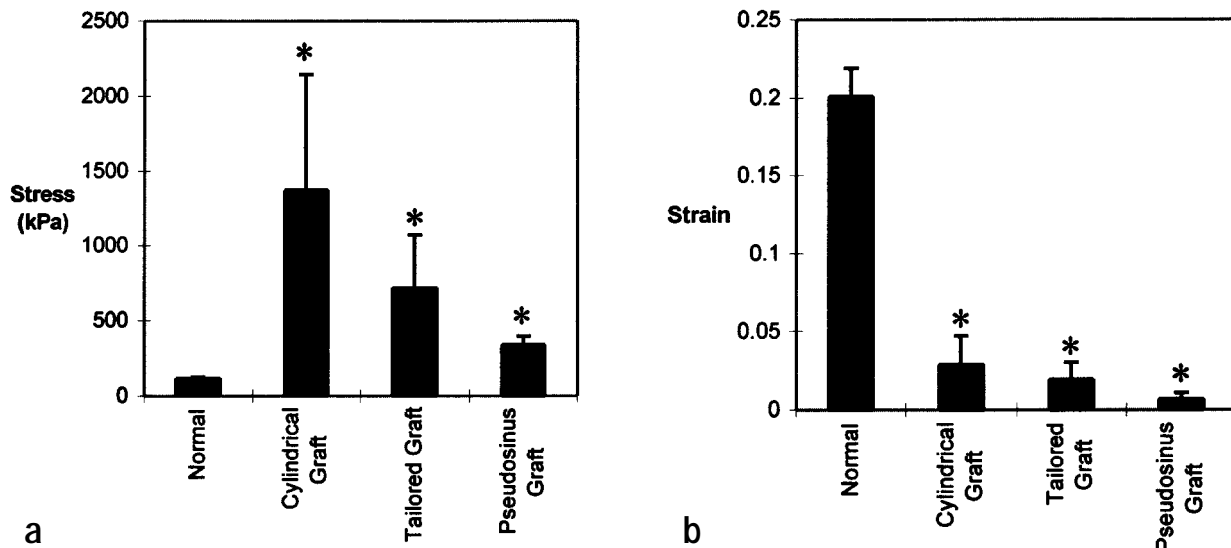


Fig 8. Sinus wall stresses (a) and strains (b) in the normal root and clinical valve-sparing models. Asterisk (*) indicates significant difference as compared with the normal root model.

been reported to function in the linear, higher stiffness region of its stress-strain function.^{15,26} Third, the stress analysis was based on the assumption that the zero-pressure state in the root and valve at the start of model solution was equivalent to a zero-stress state. Because of residual stresses caused by the differential makeup of the valve and aortic wall layers^{17,27} and dynamic motion throughout the cardiac cycle, a zero-stress state may not exist in vivo. We assumed that the magnitude of these residual stresses would be negligible in comparison with the valve and root stresses at peak valve pressure. Fourth, a small-deformation analysis, rather than large-deformation analysis, was used. Our rationale for this approach was that the applied simulated pressures did not lead to significant changes in the model geometry. We therefore assumed that any incrementally increased deformations that could be gained from a large deformation analysis would not be large enough to justify the extra computational burden.

Despite these limitations, the different graft models used identical physiologic loading conditions; only specific material properties and root geometry were altered. Therefore comparison between models provides a *relative* estimate of the stress and strain differences that could be expected in vivo due to aortic root replacement with a vascular graft.

Graft influence on leaflet stress, strain, and coaptation. All three graft models altered the normal stress, strain, and coaptation patterns as compared with the normal model. In the cylindrical model, diastolic leaflet stresses and strains were predominantly increased at the attachment edge and belly, the two

leaflet regions closest to the graft. These regions are already subject to high bending and flexural stresses during leaflet opening,²⁶ and further increases in stress during closure could be damaging. Stresses in the leaflet coaptation area and free margins were less affected because of the increased leaflet coaptation, which provided those regions with compressive stress relief. However, this increased coaptation is a result of the simulated valve functioning within a smaller space than normal (the stiff polyester graft). The resultant potential for leaflet folding and buckling would likely cause leaflet damage in the clinical setting and may significantly reduce the durability of the procedure. The incremental improvement in leaflet stresses, strain, and coaptation in the tailored graft model as compared with the original cylindrical model is related to the graft having been “trimmed” to have a simulated attachment *above* the crown-shaped valve annulus. The lack of circumferential restriction around the remaining aortic root provided an increased freedom of movement at the commissures. The pseudosinus graft model resulted in the lowest stress levels in the valve and sinus walls of all the graft models. Although leaflet stresses were still increased at the attachment edge, the relatively normal stresses in the central leaflet areas in this graft model reflect the more normal coaptation as a result of the narrowed upper sinus diameter. Overall, these models suggest that although selected graft tailoring styles may perform relatively better than the original cylindrical graft, the rounded shape of the root wall (as created by the pseudosinus graft procedure) is

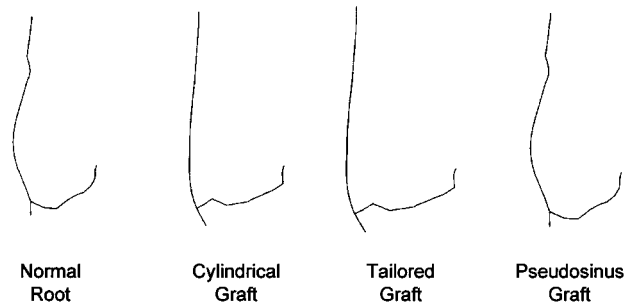


Fig 9. Cross-sections of the noncoronary sinus wall–valve leaflet functional unit in the normal root and three polyester graft models.

more suitable to share the pressure-induced load with the leaflets than the cylindrical or tailored graft.

Graft influence on root–valve relationship. These changes in leaflet stress, strain, and coaptation indicate a departure from the normal aortic root–valve relationship, in that the definitive shape of the valve–root sinus functional unit has been changed. As described by Thubrikar and associates⁵ each leaflet and corresponding sinus wall comprise a cylindrically shaped functional “unit” with continuity between the leaflets and root to distribute the diastolic pressure load. In this manner, the aortic valve transfers the high attachment edge stresses from the leaflet to the lower-stiffness root wall. This stress transfer appeared to be reversed in the graft models, where high stresses in the grafts were transferred to the valve, thereby increasing the overall leaflet stresses. Additionally, the functional unit represented by the sinus wall and leaflet together in these models was not cylindrically shaped (Fig 9). The changes to the root–valve relationship in the pseudosinus model were not as pronounced as that in the cylindrical and tailored models.

Implications for graft use in valve-sparing procedures. Despite different trimming techniques to provide the graft with a rounded sinus-like shape, all these methods are applied to the same class of polyester material grafts. Because the elastic modulus of polyethylene terephthalate is an order of magnitude greater than that of the normal aortic root,^{16,28} concern has been expressed that the use of this material might transfer high stresses to the spared aortic valve, perhaps reducing the durability of a surgical valve repair. In our finite element models of valve sparing, the woven polyester graft did not fully restore the normal aortic valve environment. However, optimization of vascular graft design involves a greater number of variables than simply shape and material properties (ie, biocompatibility considerations). Future finite element modeling may

provide additional evaluation of alternative material choices and may contribute to the eventual design of a “mechanically biocompatible” aortic root graft.

Conclusion

We conclude that valve-sparing root replacement techniques that do not re-create the normal sinus space (the cylindrical graft) result in higher than normal leaflet stresses in our finite element models. Our findings suggest that techniques that allow the potential for sinus space formation (the tailored cylindrical graft and, particularly, the pseudosinus graft) bring leaflet stresses closer to normal.

REFERENCES

1. David TE, Feindel CM. An aortic valve–sparing operation for patients with aortic incompetence and aneurysm of the ascending aorta. *J Thorac Cardiovasc Surg* 1992;103:617-21; discussion 622.
2. Cochran RP, Kunzelman KS, Eddy AC, Hofer BO, Verrier ED. Modified conduit preparation creates a pseudosinus in an aortic valve–sparing procedure for aneurysm of the ascending aorta. *J Thorac Cardiovasc Surg* 1995;109:1049-57; discussion 1057-8.
3. Sarsam MA, Yacoub M. Remodeling of the aortic valve anulus. *J Thorac Cardiovasc Surg* 1993;105:435-8.
4. David TE. Aortic root aneurysms: Remodeling or composite replacement? *Ann Thorac Surg* 1997;64:1564-8.
5. Thubrikar MJ, Nolan SP, Aouad J, Deck JD. Stress sharing between the sinus and leaflets of canine aortic valve. *Ann Thorac Surg* 1986;42:434-40.
6. Bellhouse BJ, Reid KG. Fluid mechanics of the aortic valve. *Br Heart J* 1969;31:391.
7. Pourdeyhimi B, Wagner D. On the correlation between the failure of vascular grafts and their structural and material properties: a critical analysis. *J Biomed Mater Res* 1986;20:375-409.
8. Cochran R, Kunzelman K. Aortic valve sparing in aortic root disease. In: Karp D, Laks H, Wechsler A, editors. *Advances in cardiac surgery*. Vol. 8. St Louis: Mosby–Year Book; 1996. p. 81-107.
9. Christie GW, Barratt-Boyes BG. Identification of a failure mode of the antibiotic sterilized aortic allograft after 10 years: implications for their long-term survival. *J Card Surg* 1991;6:462-7.
10. Hamid MS, Sabbah HN, Stein PD. Vibrational analysis of bio-

- prosthetic heart valve leaflets using numerical models: effects of leaflet stiffening, calcification, and perforation. *Circ Res* 1987; 61:687-94.
11. Grande KJ, Cochran RP, Reinhall PG, Kunzelman KS. Stress variations in the human aortic root and valve: the role of anatomic symmetry. *Ann Biomed Eng* 1998;26:534-45.
 12. Zienkiewicz O, Cheung Y. The finite element method in structural and continuum mechanics: numerical solution of problems in structural and continuum mechanics. 1st ed. London: McGraw-Hill; 1967.
 13. Clark RE, Finke EH. Scanning and light microscopy of human aortic leaflets in stressed and relaxed states. *J Thorac Cardiovasc Surg* 1974;67:792-804.
 14. Sahasakul Y, Edwards WD, Naessens JM, Tajik AJ. Age-related changes in aortic and mitral valve thickness: implications for two-dimensional echocardiography based on an autopsy study of 200 normal human hearts. *Am J Cardiol* 1988;62:424-30.
 15. Dobrin PB. Vascular mechanics. In: Shepherd JT, Abboud F, editors. *Handbook of physiology*. Vol. 3. Washington, DC: American Physiological Society; 1983. p. 65-102.
 16. Kalath S, Tsipouras P, Silver FH. Non-invasive assessment of aortic mechanical properties. *Ann Biomed Eng* 1986;14:513-24.
 17. Vesely I, Noseworthy R. Micromechanics of the fibrosa and the ventricularis in aortic valve leaflets. *J Biomech* 1992;25:101-13.
 18. Vawter DL. Poisson's ratio and incompressibility. *J Biomech Eng* 1983;105:194-5.
 19. Vesely I, Boughner D. Analysis of the bending behaviour of porcine xenograft leaflets and of neutral aortic valve material: bending stiffness, neutral axis and shear measurements. *J Biomech* 1989;22:655-71.
 20. McGiffin DC, McGiffin PB, Galbraith AJ, Cross RB. Aortic wall stress profile after repair of coarctation of the aorta: Is it related to subsequent true aneurysm formation? *J Thorac Cardiovasc Surg* 1992;104:924-31.
 21. Abbott WM, Cambria RP. Control of physical characteristics (elasticity and compliance) of vascular grafts. In: Stanley JC, editor. *Biologic and synthetic vascular prostheses*. New York: Grune & Stratton; 1982. p. 59-78.
 22. Edwards WS, Snyder RW, Botzko K, Larkin J. Comparison of durability of tensile strength of Teflon and Dacron grafts. In: Dardik H, editor. *Graft materials in vascular surgery*. Chicago: Symposia Specialists Inc; 1978. p. 169-82.
 23. Kidson IG. The effect of wall mechanical properties on patency of arterial grafts. *Ann R Coll Surg Engl* 1983;65:24-9.
 24. King MW, Guidoin RG, Gunasekera KR, Gosselin C. Designing polyester vascular prostheses for the future. *Med Prog Technol* 1983;9:217-26.
 25. Han HC, Fung YC. Longitudinal strain of canine and porcine aortas. *J Biomech* 1995;28:637-41.
 26. Thubrikar M, Piepgrass WC, Deck JD, Nolan SP. Stresses of natural versus prosthetic aortic valve leaflets in vivo. *Ann Thorac Surg* 1980;30:230-9.
 27. Fung YC. *Biomechanics: mechanical properties of living tissues*. 2nd ed. New York: Springer-Verlag; 1993.
 28. Abbott WM, Bouchier-Hayes DJ. The role of mechanical properties in graft design. In: Dardik H, editor. *Graft materials in vascular surgery*. Chicago: Symposia Specialists Inc; 1978. p. 59-78.

Commentary

Dr Grande-Allen and colleagues used finite element analysis to compare the stress and strain on the aortic

cusps in normal aortic roots and in surgically reconstructed roots by means of aortic valve-sparing operations. They used magnetic resonance imaging of normal human aortic roots to establish the geometry of the model for their finite element analysis and made theoretical assumptions on three types of aortic root reconstruction with preservation of the native aortic cusps and anulus. They assumed that the technique of reimplantation of the aortic valve^{1,2} creates a "cylindrical" aortic root of Dacron fabric without sinuses, the technique of remodeling of the aortic root^{1,2} creates a supra-annular "cylinder" of Dacron fabric without aortic sinuses, and finally the technique of reimplantation of the aortic valve into a Dacron graft with a scalloped subannular suture line creates three "pseudosinusus."³ Although the aortic cusps in all three theoretical models of reconstructed aortic root had increased stress and strain when compared with the normal aortic root, the first technique was associated with the highest and the one with neo-aortic sinuses with the lowest stress and strain. Those investigators concluded that "valve-sparing techniques that allow the potential for sinus space formation (tailored, pseudosinus) result in simulated leaflet stresses that are closer to normal than the cylindrical technique."

In addition to the limitations of the study pointed out by the authors, another important limitation was the theoretical assumptions on the geometry of the reconstructed aortic roots after various types of aortic valve-sparing operations. They used magnetic resonance images of human aortic roots to create the "normal" model for the finite element analysis and used their imagination to create the models of the reconstructed roots. Had they used magnetic resonance or echocardiographic images of reconstructed aortic roots, the results would have been quite different. More important, the results would vary from patient to patient depending on who had the same type of aortic root reconstruction.

I have had no clinical experience with the third type of reconstruction of the aortic root these authors described,³ but I have reconstructed almost 200 aortic roots using the techniques of reimplantation of the aortic valve and remodeling of the aortic root.¹⁻² During the first few years of my experience with these operations, I used almost exclusively the technique of reimplantation of the aortic valve. Then I met one of the investigators of this study, Dr Karyn Kunzelman, who convinced me that the aortic sinuses were important for normal aortic valve closure and possibly durability,¹ and I began to use the technique of remodeling of the aortic root. Contrary to hypothetical geometric models of reconstructed roots described by Dr Grande-Allen and colleagues,

remodeling of the aortic root creates three neo-aortic sinuses when correctly performed. The areas of these neo-aortic sinuses depend on the height of the tailored portion of the tubular graft. The more graft used to suture along the scalloped shape of the aortic annulus, the more neo-aortic sinus is obtained. When this technique is used, the resulting echocardiographic image of the reconstructed root resembles that of a normal aortic root. Thus, if geometry of the aortic sinuses is important for cusp stress and strain, this technique should offer the best results.

Creation of neo-aortic sinuses is also feasible when the technique of aortic valve reimplantation is used. One of the most difficult aspects of these operations is the selection of graft size. I have always used a graft larger than what I think is necessary. After discontinuation of cardiopulmonary bypass, the motion and function of the aortic cusps are assessed by echocardiography. If there is central regurgitation or the leaflets do not coapt properly, it is possible to correct the problem by adjusting the diameter of the sinotubular junction of the reconstructed aortic root. If the cusps move normally, a space between them and the graft wall is almost invariably present and can be documented intraoperatively by M-mode echocardiography.

It is possible that reimplantation of the aortic valve into a tubular Dacron graft increases the stress and strain on the aortic cusps, but after 12 years of clinical experience with aortic valve-sparing operations, reimplantation of the aortic valve has provided the most durable and event-free survival of all aortic valve-sparing operations I have performed.

This operation is easier to perform and it is reproducible by other surgeons. Remodeling of the aortic root requires greater knowledge of the functional anatomy of the aortic root, and the results may be more dependent on the surgeon's ability to restore normal aortic root anatomy using a tailored tubular graft.

*Tirone E. David, MD
Toronto, Ontario, Canada*

REFERENCES

1. David TE, Feindel CM, Bos J. Repair of the aortic valve in patients with aortic insufficiency and aortic root aneurysm. *J Thorac Cardiovasc Surg* 1995;109:345-52.
2. David TE. Remodeling of the aortic root and preservation of the native aortic valve. *Op Tech Card Cardiovasc Surg* 1996;1:44-56.
3. Cochran RP, Kunzelman KS, Eddy AC, Hofer BO, Verrier ED. Modified conduit preparation creates a pseudosinus in an aortic valve-sparing procedure for aneurysm of the ascending aorta. *J Thorac Cardiovasc Surg* 1995;109:1049-57.

12/1/104875

doi:10.1067/mtc.2000.104875